

Extraction of T_1/T_2 Relaxation Times of Glycerine and Copper Sulfate Solution via Pulsed Nuclear Magnetic Resonance

Rio Weil*

Department of Physics, University of Chicago, Chicago, Illinois 60637, USA

(Dated: April 25, 2025)

We apply pulsed nuclear magnetic resonance techniques to probe the magnetic properties of glycerine, teflon, and aqueous copper samples. We measure the gyromagnetic ratio of hydrogen to be $\gamma_H = 41.29(33)\text{MHz}\cdot\text{T}^{-1}$ and that of fluorine to be $\gamma_F = 39.25(30)\text{MHz}\cdot\text{T}^{-1}$. We measure the T_2 (spin-lattice) relaxation time of Glycerine to be $T_1 = 41.16(47)\text{ms}$ and the T_2 (spin-spin) relaxation time to be $T_2 = 25.55(90)\text{ms}$. We prepare copper solutions of varying concentrations from 10^{-1} - 10^{-5}mol/L and analyze the dependence of T_1 and T_2 times on ion concentration, fitting the former with a power law with best fit power of $n = -0.7920(14)$ and the latter with logarithmic scaling with semi-log slope of $m = -7.11(13)$. Both fits are of poor quality, suggesting that our data is not able to well-characterize the dependence of relaxation time on ion concentration. Comparing our results to established literature values for gyromagnetic ratios and relaxation times shows statistically significant disagreement, and we discuss potential sources of systematic error in our experiments that could explain such discrepancies.

I. INTRODUCTION

Nuclear Magnetic Resonance, or NMR is a spectroscopic technique for studying magnetic nuclei in a constant magnetic field via their resonance response to an oscillating radiofrequency field. The technique was initially pioneered in the late 1940s by Purcell [1] [2], Bloch [3], and Hahn [4] for the experimental study of condensed matter systems. It has since been extended to spectroscopy of soft matter systems, to non-invasively measure water content [5], and perhaps most importantly in magnetic resonance imaging [6].

In this paper, we employ pulsed NMR (first discovered by Hahn [4], now the leading technique in the field), using the inversion recovery and spin echo methods to probe the relaxation times of glycerine and copper samples. We are in particular interested in asking how relaxation times scale with ion concentration. Though we do not study a biologically abundant ion (copper), an understanding of this scaling could nevertheless be relevant in the application of NMR to biological systems, where differing concentrations of ions across tissue can be leveraged for high-contrast medical imaging.

The rest of this paper is organized as follows. In Section II we discuss the basic theory of NMR through review quantum mechanics for spin-1/2 systems, and introduce notions of the gyromagnetic ratio and T_1 & T_2 relaxation times. In III we introduce the experimental apparatus and discuss how the relaxation time measurements were conducted using the inversion recovery and spin echo techniques. In Section IV we discuss the measurement of the gyromagnetic ratio of Hydrogen and Fluorine nuclei. In Section V we discuss the measurement of the T_1 and T_2 relaxation times for glycerine. In Section VI we discuss the preparation and relaxation time

measurements for solutions of variable copper ion concentration and attempt to extract the dependence of T_1/T_2 times on ion concentration. In Section VII we conclude.

II. THEORY

A. Dynamics of a spin-1/2 system in a magnetic field

To understand the physical mechanism for the resonance response of nuclei, we begin with an analysis of a spin-1/2 particle (here, a proton) in an external magnetic field $\mathbf{B} = B_0\hat{\mathbf{z}}$. This system has Hamiltonian:

$$H = -\gamma \frac{\hbar}{2} B_0 \sigma_z \quad (1)$$

and corresponding eigenstates $|\pm\rangle$ with energies $E_{\pm} = \pm\gamma\frac{\hbar}{2}B_0$. The energy splitting between the two states is then:

$$\Delta E =: \hbar\omega_0 = \hbar\gamma B_0 \quad (2)$$

where we have defined the Larmor/resonance frequency $\omega_0 = \frac{\Delta E}{\hbar}$, which is the frequency of precession in the xy-plane for state $\frac{1}{\sqrt{2}}(|+\rangle + |-\rangle)$. The γ factor appearing in the above discussion is the *gyromagnetic ratio*, which is a nuclei-dependent quantity which can be measured as the ratio of a nuclei resonant frequency with the strength of the static \mathbf{B} -field:

$$\gamma = \frac{\omega_0}{B_0}. \quad (3)$$

To drive transitions in between the $|\pm\rangle$ states, we consider the addition of a radiofrequency (RF) field that rotates in time[7] with frequency ω :

$$\mathbf{B}(t) = B_0\hat{\mathbf{z}} + B_1(\cos(\omega t)\hat{\mathbf{x}} + \sin(\omega t)\hat{\mathbf{y}}) \quad (4)$$

* ryoheiweil@uchicago.edu

This system can be solved exactly, and the probability of spin flips from the ground state $|-\rangle$ to the excited state $|+\rangle$ can be found to be [8]:

$$P_{- \rightarrow +}(t) = \frac{B_1^2 \gamma^2}{B_1^2 \gamma^2 + (\omega - \omega_0)^2} \sin^2 \left[\left(\frac{\gamma^2 B_1^2 + (\omega - \omega_0)^2}{4} \right)^{1/2} t \right] \quad (5)$$

such spin flips are known as Rabi oscillations, and it can be seen that at resonance:

$$\omega = \omega_0 \quad (6)$$

the probability for spin flips is maximized. Thus, we may apply time-dependent radiofrequency fields to a sample of magnetic nuclei in order to induce spin flips, in addition to the dynamics of precession as induced by a constant magnetic field.

B. Thermodynamics of ensembles of spins

The magnetic field arising from an individual spin in any sample of magnetic nuclei is impossible to measure - instead, we are interested in the net magnetization as obtained from the sum of the individual magnetizations \mathbf{m}_i :

$$\mathbf{M} = \sum_i \mathbf{m}_i \quad (7)$$

Therein, it is relevant to consider the fraction of the two spin populations N_+ (higher energy/anti-aligned) and N_- (lower energy/aligned) at thermal equilibrium, which is given by the Boltzmann distribution:

$$\frac{N_+}{N_-} = \exp\left(-\frac{\Delta E}{k_B T}\right) = \exp\left(-\frac{\hbar\omega_0}{k_B T}\right) \quad (8)$$

The deviation of the above ratio from one[9] allows for the observation of the net magnetization:

$$M_z = \mu(N_- - N_+). \quad (9)$$

We will be interested in manipulating/observing this net magnetization, and its timescales of relaxation.

C. T1 (Spin-Lattice) Relaxation

The T_1 , or spin-lattice relaxation time is the time constant for the exponential relaxation of the magnetization on the z -axis (aligned with the constant magnetic field). It can be measured by inverting the equilibrium net magnetization via RF pulse (such that the magnetization is antiparallel to the static field), and then measuring the relaxation time back to the equilibrium magnetization. In particular, the rate at which the system approaches equilibrium is proportional to the distance from equilibrium and inversely proportional to the T_1 time, and so:

$$\frac{dM_z}{dt} = \frac{M_0 - M_z}{T_1} \quad (10)$$

which can be solved to obtain the magnetization as a function of time (assuming an inverted magnetization at the initial time, $M_z(t=0) = -M_0$):

$$M_z(t) = M_0(1 - 2e^{-t/T_1}) \quad (11)$$

D. T2 (Spin-Spin) Relaxation

In addition to the relaxation of the z -magnetization, there is also a relaxation of magnetization in the xy plane, characterized by the T_2 time. If we rotate the equilibrium magnetization into the xy -plane, the protons all would exhibit Larmor precession in phase and so the xy -magnetization would stay fixed in time. However, in a physical ensemble of protons, the magnetic field felt by individual protons varies due to interactions with the dipole fields of their neighbors. Hence the initially in-phase protons precess at different rates, with the proton precession becoming increasingly out of phase in time, with the xy -magnetization eventually dropping to zero. The rate of the relaxation is proportional to the x/y magnetization at a given time and inversely proportional to the T_2 time, so:

$$\frac{dM_{x/y}}{dt} = -\frac{M_{x/y}}{t} \quad (12)$$

which can be solved to obtain:

$$M_{x/y}(t) = M_0 e^{-t/T_2} \quad (13)$$

III. APPARATUS + DATA COLLECTION

Our experimental setup consists of a static large magnet and associated controls, Helmholtz coils to induce a time-dependent magnetic field and the associated RF pulse controller, an induction coil, receiver and signal mixer for obtaining and processing the output signal, and an oscilloscope for display and readout of the output. This is depicted in Fig. 1.

A more detailed diagram of the magnet and sample location is given in Fig. 2. The static magnetic field points in the \hat{z} direction. The Helmholtz coils produce a time-varying RF field in the y -direction. In particular, we are interested in two specific types of RF pulses - namely a 90 degree pulse to rotate the magnetization from $M_z \rightarrow M_y$, or a 180 degree pulse to rotate the magnetization from $M_z \rightarrow -M_z$. The receiver coil then picks up the magnetization M_x in the \hat{x} direction, converted into an electrical signal sent to the receiver.

A. Procedure for Measuring T1

We can establish the resonance frequency ω_0 of the nuclei in the sample as follows. We set an RF frequency ω

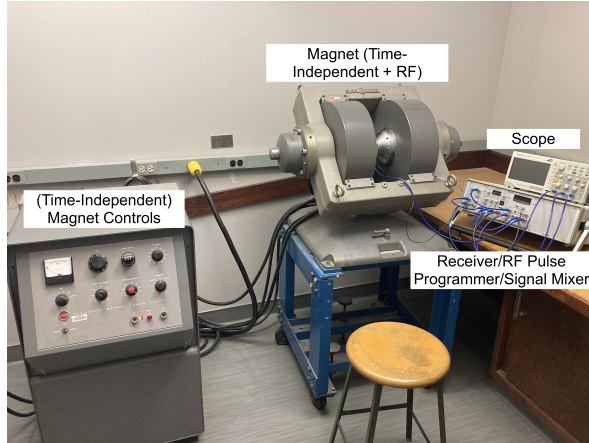


FIG. 1. Diagram of the broad experimental setup.

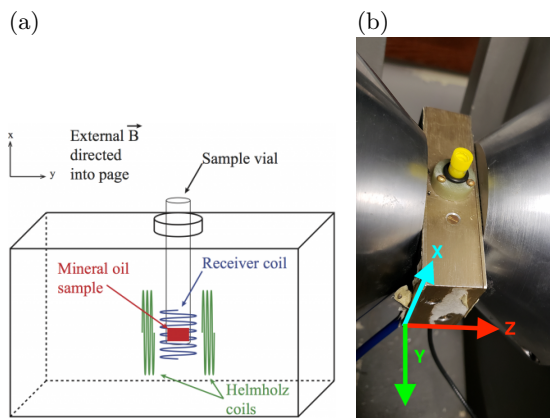


FIG. 2. (a) Cartoon diagram of the sample vial. The static magnetic field points in \hat{z} , while the Helmholtz coil generates an RF field in \hat{y} . The \hat{x} is read out and output by the receiver coil. (b) Picture of sample vial and detector block. Both figures were taken from [10].

and apply a 90 degree pulse to the sample at this frequency. We can then vary the static field strength B_0 , which changes the precession frequency of nuclei in the sample. Recalling our analysis of the Rabi oscillation formula, when the precession frequency $\omega_0 = \gamma B_0$ is close to the RF frequency ω , the spins are maximally rotated into the xy -plane, causing a spike in the output and subsequent decay of the xy -magnetization. This is the free induction decay (FID) signal as shown in Fig. 3. To obtain a more precise resonance signal, the oscillating signal of the precessing protons can be added to the RF frequency through use of the signal mixer. This superimposed signal will exhibit beats with frequency $f_B = \omega - \omega_0$, and by tuning this beat frequency to zero we can establish that the sample is on resonance.

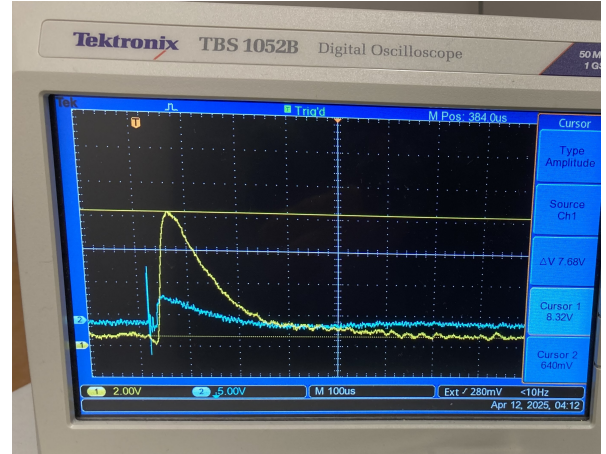


FIG. 3. Free induction decay curve displayed on oscilloscope (yellow). By rotating the equilibrium magnetization into the xy -plane with a 90° RF pulse on resonance ($\omega = \omega_0$), we see a spike in the x -magnetization (followed by decay due to spin-spin interactions, as well as magnet field inhomogeneities). Also displayed is the signal mixer output (blue) which is the superposition of the output signal and the RF frequency. Here, we have tuned the beat frequency $f_B = \omega - \omega_0$ to zero, indicating that we are on resonance.

B. Procedure for Measuring T_1

For a given sample, we use the inversion recovery method for measuring the T_1 time is as follows.

1. Tune the magnetic field/RF frequency to resonance, as is discussed in the previous section.
2. Wait for the sample to relax to the equilibrium magnetization. This is set by the repetition time. Then, apply the following pulse sequence:
 - (a) At $t = 0$, apply a 180° RF pulse to invert the equilibrium magnetization \hat{z} to $-\hat{z}$.
 - (b) Wait for delay time τ .
 - (c) At time $t = \tau$, apply a 90° RF pulse to rotate the magnetization vector into the xy plane. The signal is then read out by the readout coil.
3. Measure the output FID signal amplitude ΔV on the scope (which is proportional to the z -magnetization at time t) as the difference between the baseline and FID peak.
4. Repeat steps 2-3 for multiple delay times τ , and extract T_1 through fitting the amplitude data to:

$$M_z(t) = M_0(1 - 2e^{-t/T_1}) \quad (14)$$

C. Procedure for Measuring T_2

The extraction of T_2 is more subtle than that of T_1 . Namely, there are two effects we want to isolate when we

study the dephasing of the magnetization in the xy -plane. The magnetic field inhomogeneities that cause the local variations in precession frequency can arise both from (a) the neighbouring spins, as well as (b) from magnetic field inhomogeneities in the sample (the decay of the magnetization as shown in the FID curve of Fig. 3 is due to both of these effects combined - this decay time is sometimes known as the T_2^* time). The former corresponds to the property of the sample we wish to measure, and the latter is a setup-specific effect to compensate. To this end, we use the spin echo method:

1. Tune the magnetic field/RF frequency to resonance, as is discussed in the previous section.
2. Wait for the sample to relax to the equilibrium magnetization. This is set by the repetition time. Then, apply the following pulse sequence:
 - (a) At $t = 0$, apply a 80° RF pulse to invert the equilibrium magnetization \hat{z} into the xy -plane.
 - (b) Wait for delay time τ .
 - (c) At time $t = \tau$, apply a 180° RF pulse to flip the magnetizations.
 - (d) Wait for delay time τ
 - (e) A spin echo signal is then produced, and output by the readout coil.
3. Measure the output spin echo amplitude ΔV on the scope (which is proportional to the x/y -magnetization at time 2τ) as the difference between the baseline and spin echo peak.
4. Repeat steps 2-3 for multiple delay times τ , and extract T_2 through fitting the amplitude data to:

$$M_z(t) = M_0 e^{-\frac{t}{T_2}} \quad (15)$$

The spin echo signal is shown in Fig. 4. This procedure allows us to compensate for inhomogeneities in the magnetic field due to the inversion step. If nuclei precess more quickly/slowly due to such inhomogeneities, in the 180° pulse inversion step they are flipped, and another delay time later the precessing nuclei again catch up and superimpose, forming the spin echo peak. The amplitude of the spin echo peak is thus only dependent on the decay of the xy -magnetization due to spin-spin interactions (which are irreversible), and thus tracking its decay as a function of (twice the) delay time yields a measure of T_2 .

To estimate the uncertainty in our ΔV measurements (both for FID and spin echo peaks), we observed the voltage range over which the peak height and the baseline vary (on the order of $\sim 0.8V$, due to the amplification of electrical noise) through multiple measurement cycles. We then took the maximum/minimum as the approximate bounds of a 95% confidence interval for the voltage measurement, and divided the range by 4 to approximate one σ . We then added the uncertainty from

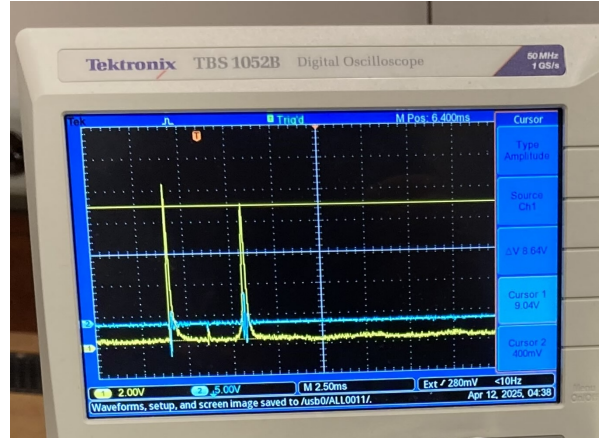


FIG. 4. Spin echo signal displayed on oscilloscope (yellow). At $t = 0$ a 90° pulse is applied, causing a FID signal. At time $t = \tau$, we apply a 180° pulse (as seen as the blip in between the peaks), inverting the precessing spins in the xy -plane. At time $t = 2\tau$, we then observe the spin echo peak from the variable-frequency precessing spins reconstituting.

the peak and baseline, as well as the uncertainty arising from instrumental resolution ($0.04V$, half of the smallest digital step of the scope) in quadrature to obtain the uncertainty in the amplitude. This statistical uncertainty is what is depicted in the error bars of the plots in the following sections. Uncertainties in delay times were taken to be half of the smallest digit of the programmer ($\delta t = .05s/0.5s/5s$) depending on the relaxation times being probed. Relative uncertainties in the delay times are small, and we neglect them in the proceeding plots as they are always so small as to be hidden behind data markers.

IV. MEASUREMENTS OF GYROMAGNETIC RATIOS

To measure the gyromagnetic ratio of the nuclei in our samples, we first set the RF frequency to 15.4MHz for a single pulse (we neglect the associated instrumental uncertainty, as the RF frequency is precise to 10Hz). We then tune the static field strength to resonance, as is discussed in section III. We then use a DC gaussmeter to measure the magnetic field strength. We first calibrate the gaussmeter to a reference magnetic field of 999 Gauss, then measure the field strength at the location of the sample. We find a calibration offset of $+220(2)$ Gauss, and for Glycerine measure a static field strength of $3509(30)$ Gauss. The uncertainty in the magnetic field reading is estimated by approximating the 95% confidence interval ($\pm 2\sigma$) as the maximum/minimum of temporal fluctuations of the Gaussmeter reading, and dividing by four. We can then subtract off the calibration offset to obtain the value of B_0 at resonance, and take the ratio with the frequency to obtain the gyromag-

Nuclei	Measured ($\text{MHz} \cdot \text{T}^{-1}$)	Literature($\text{MHz} \cdot \text{T}^{-1}$)	t'
Hydrogen	41.29(33)	42.577478518(18)	3.9
Fluorine	39.25(30)	40.069244(61)	2.5

TABLE I. Comparison of gyromagnetic ratios of hydrogen (glycerine sample) and fluorine (teflon sample) compared with literature values [11] from IAEA and CODATA.

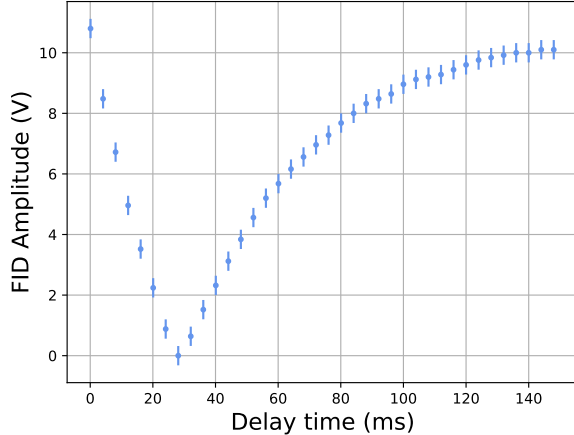


FIG. 5. FID amplitude vs. delay time for Glycerine. Repetition time was set as 1 second. Error bars are statistical. Positive FID amplitudes were measured for $\tau < 24\text{ms}$, though the magnetization of the sample is negative.

netic ratio. Performing this for hydrogen (glycerine) and fluorine (teflon) nuclei, we obtain the results in Table I.

For both hydrogen and fluorine, we obtain gyromagnetic ratios that are of the correct order of magnitude, but show statistical disagreement/tension with accepted literature values. Since both the hydrogen and fluorine nuclei display similar offsets, this suggests that there is a systematic error in the magnetic field or frequency measurements. The most likely explanation is that there was an error in calibration of the DC gaussometer. A future measurement could improve the calibration procedure by measuring against several known magnetic field strengths, and help to resolve the statistical disagreement we observe.

V. RELAXATION TIMES OF GLYCERINE

All proceeding T1, T2 data was collected at a RF frequency of 15.4MHz, with a measured field strength of $B_0 \sim 0.37\text{T}$ and at room temperature of $T \sim 293\text{K}$.

Following the procedure in Section III, we measure the FID peak amplitude as a function of the delay time between the 180 and 90 degree pulses. For the 100% Glycerine sample, we find the amplitude vs. time curve given in Fig. 5.

The amplitude of the FID curve is unsigned, and therefore cannot discriminate between magnetization in the $\pm\hat{\mathbf{z}}$ directions. However, since the $\hat{\mathbf{z}}$ -magnetization

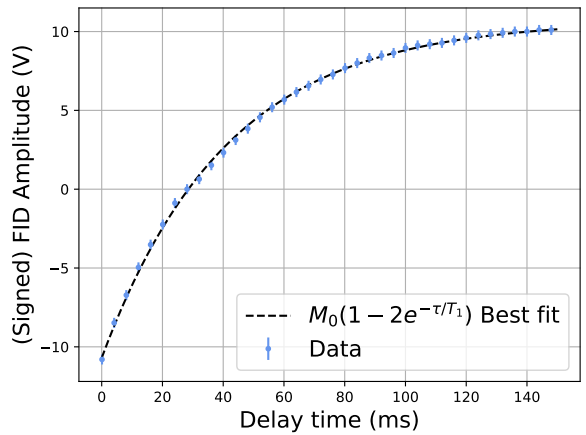


FIG. 6. FID amplitude vs. delay time for Glycerine and associated fit for extracting T_1 . Repetition time was set as 1 second. Error bars are statistical. The best fit parameters were $T_1 = 41.16(47)\text{ms}$ and $M_0 = 10.703(91)\text{V}$, with a reduced chi-squared of $\chi_{\text{red}}^2 = 0.24$.

is a monotonically increasing function of time towards the equilibrium value, we can infer that the magnetization immediately after the inversion/180° pulse is negative, and that it remains negative until the amplitude reaches zero. Hence, we may interpret the amplitudes for $\tau < 24\text{ms}$ in Fig. 5 as corresponding to negative magnetization, and therefore flip its sign. We perform this data processing step for all proceeding T_1 extractions. With this step, we reproduce the expected form of the decay curve, which can be fit by the model given in Eq. (14). This is shown in Fig. 6.

The model appears to fit the data well, though the reduced-chi squared suggests that the uncertainties may have been slightly overestimated. The least squares fit yields a T_1 value of $T_1 = 41.16(47)\text{ms}$. A comparison with the measured value for glycerol [12] of $T_1 = 21.1(46)\text{ms}$ taken at similar experimental parameters of $B_0 = 0.35\text{T}$ and $\omega_0 = 14.71\text{MHz}$ leads to a $t' = 4.3$, indicating statistically significant disagreement.

Now following the spin echo procedure in Section III, we measure the spin echo amplitude as a function of the delay time between the 90 and 180 degree pulses, and we find the amplitude vs. time curve given in Fig. 7.

Again the model appears to fit the data well, with the reduced-chi square again suggesting that uncertainties may have been overestimated.

The reduced-chi squared suggests that the uncertainties may have been slightly overestimated. The least squares fit yields a T_2 value of $T_2 = 25.55(90)\text{ms}$. A comparison with the measured value for glycerol in [12] of $T_2 = 13.95(36)\text{ms}$ leads to a $t' = 12.0$, indicating statistically significant disagreement.

In both cases, we suspect (particularly given the goodness of fit of the T_1/T_2 decay model functions to the data) that the statistical discrepancy may arise due to a difference in sample purity. The samples of glycerine prepared

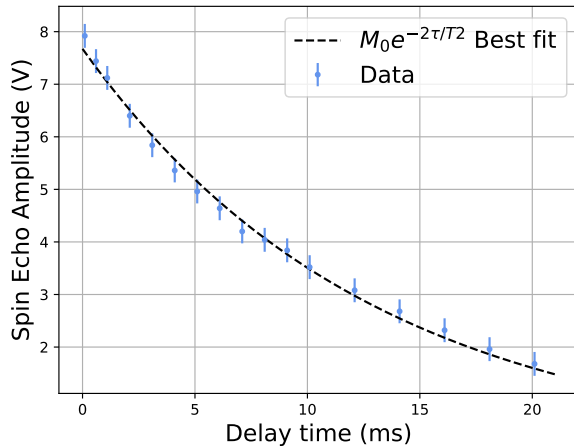


FIG. 7. Spin echo amplitude vs. delay time for Glycerine and associated fit for extracting T_2 . Repetition time was set as 1 second. Error bars are statistical. The best fit parameters were $T_2 = 25.55(90)\text{ms}$ and $M_0 = 7.67(12)\text{V}$, with a reduced chi-squared of $\chi_{\text{red}}^2 = 0.48$.

in the lab may not have been prepared with the same concentration as those used in [12]. In addition, given the hydrophilicity of glycerol, it may be possible that the purity of the samples may have degraded in time. In a future experiment, we would prepare a fresh glycerine sample and hold the purity fixed to that used in the literature experiment in order to perform a more meaningful comparison.

VI. RELAXATION TIMES OF AQUEOUS COPPER SOLUTIONS

A. Sample Preparation

To prepare solutions with varying concentrations of copper, we dissolved solid copper sulfate (CuSO_4) into deionized water, ensuring the solution was well-mixed via a magnetic stirrer. To prepare a 0.1 mol/L solution, we weigh out the solid according to:

$$m = cV\rho \quad (16)$$

where $c = 0.1\text{mol/L}$ is the concentration, $V = 100\text{mL}$ is the target volume, and $\rho = 159.6\text{g/mol}$ is the molar mass of CuSO_4 .

Following this procedure, we weighed out $1.600(5)\text{g}$ of CuSO_4 and dissolved it in $100.020(5)\text{g}$ of water, producing a $c = 0.10023(32)$ mol/L concentration solution. To produce subsequent concentrations (in dilution factors of 10) we combine 1 part of the previous concentration with 9 parts deionized water. Iterating this procedure, we obtained 5 samples with concentrations listed in Table II. Note that since one mol of CuSO_4 contains one mol of Cu^{2+} , their molar concentrations are equivalent.

Target (mol/L)	Prepared (mol/L)
10^{-1}	$1.0023(32) \times 10^{-1}$
10^{-2}	$1.0037(49) \times 10^{-2}$
10^{-3}	$1.0027(69) \times 10^{-3}$
10^{-4}	$1.0018(84) \times 10^{-4}$
10^{-5}	$9.977(99) \times 10^{-5}$

TABLE II. Concentrations of prepared aqueous Cu^{2+} solutions. Uncertainties arise from adding the relative uncertainty arising from instrumental precision in quadrature.

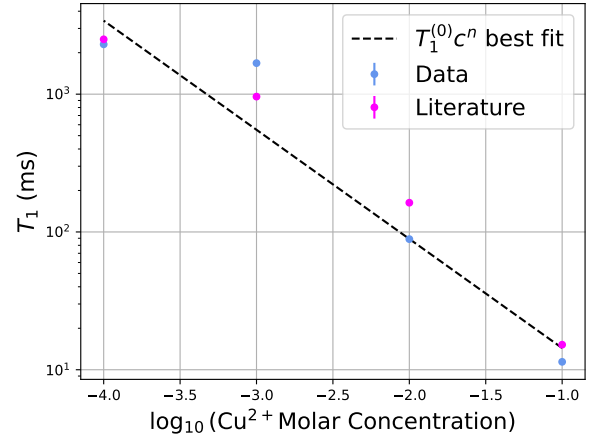


FIG. 8. T_1 relaxation time vs. Copper ion concentration, plotted alongside power law best fit and literature values from [13]. Error bars are from uncertainties in T_1 fitting parameters for individual concentration curves, and are hidden behind data markers. The best fit parameters were $n = -0.7920(14)$ and $T_1^{(0)} = 2.319(21)\text{ms}$, with a reduced chi-squared of $\chi_{\text{red}}^2 = 8926$.

B. T1 Relaxation Times

Following the procedure in Section III, we measure the FID peak amplitude as a function of the delay time between the 180 and 90 degree pulses. Doing this for the each of the copper concentrations we have created and fitting Eq. (14), we obtain the T_1 time as a function of concentration. As is suggested by the literature [13], we perform a fit to the power-law function:

$$T_1 = T_1^{(0)}c^n \quad (17)$$

where c is the concentration (normalized to be dimensionless), and the two free parameters of the fit are n (the power at which the T_1 scales) and $T_1^{(0)}$ (the T_1 time at unit concentration). The data and fit is depicted in Fig. 8.

We generally observe statistically significant disagreement with the literature values of T_1 , though the order of magnitude and the scaling of the relaxation time appears to show qualitative agreement. We also observe an extremely high value of the reduced-chi squared. Such a high value implies the obtained best-fit power-law scaling with $n = -0.7920(14)$ is not particularly meaning-

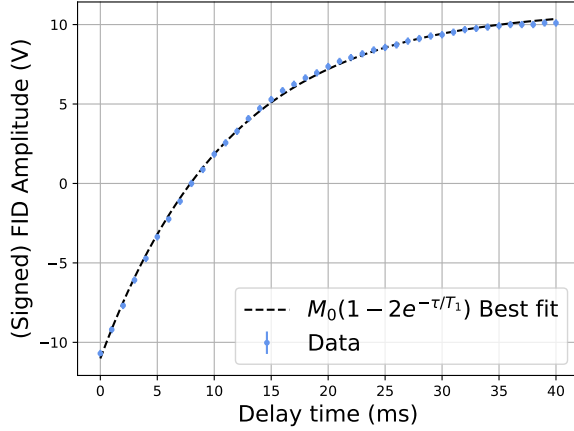


FIG. 9. FID amplitude vs. delay time for $c = 10^{-1}$ mol/L Cu^{2+} concentration solution and associated fit for extracting T_1 . Repetition time was set as 1 second. Error bars are statistical. The best fit parameters were $T_1 = 11.410(86)$ ms and $M_0 = 11.015(63)$ V, with a reduced chi-squared of $\chi_{\text{red}}^2 = 0.43$.

ful (though more datapoints would also be helpful for . The value of χ_{red}^2 suggests that the uncertainty in the T_1 points may be underestimated.

However, studying the individual concentration curves across Fig. 9-12, the χ_{red}^2 values which range from $0.42 - 3.67$ seem to suggest that the T_1 decay model fits the data reasonably well at each concentration. We do note that the $c = 10^{-2} - 10^{-4}$ curves indicate a slight systematic deviation from the best fit T_1 decay curve. In particular, in the $c = 10^{-3}/10^{-4}$ curves we see a discontinuity in the signed amplitude values at the midpoint of the curves. This occurred due to the amplitude not decaying to zero completely at any value of the delay time, and instead saturating at a finite value before increasing. This seems to suggest that the $\hat{\mathbf{z}}$ -magnetization never decays to zero for these concentrations, suggesting a systematic effect that causes the magnetization to not decay to zero. We suspect that this may arise due to the samples not having sufficient time to fully relax back to the equilibrium magnetization between pulse cycles. Since T_1 is on the order of multiple seconds, the maximum repetition time of 10 seconds in the pulse programmer may have been insufficient for the nuclei to fully relax. This may lead to some residual magnetization that can be observed as a systematic offset in the FID peak amplitude.

C. T₂ Relaxation Times

Following the procedure in Section III, we measure the spin echo amplitude as a function of the delay time between the 90 and 180 degree pulses. Doing this for the each of the copper concentrations we have created and fitting Eq. (15), we obtain the T_2 time as a function of

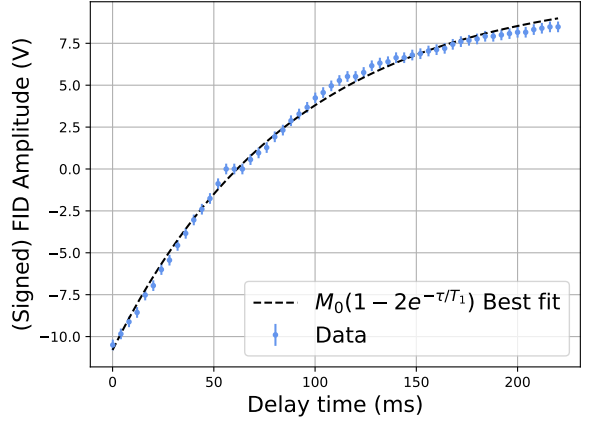


FIG. 10. FID amplitude vs. delay time for $c = 10^{-2}$ mol/L Cu^{2+} concentration solution and associated fit for extracting T_1 . Repetition time was set as 5 seconds. Error bars are statistical. The best fit parameters were $T_1 = 88.72(71)$ ms and $M_0 = 10.799(88)$ V, with a reduced chi-squared of $\chi_{\text{red}}^2 = 1.10$.

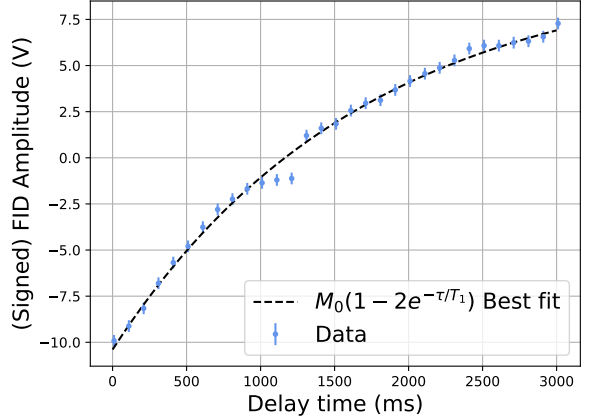


FIG. 11. FID amplitude vs. delay time for $c = 10^{-3}$ mol/L Cu^{2+} concentration solution and associated fit for extracting T_1 . Repetition time was set as 10 seconds. Error bars are statistical. The best fit parameters were $T_1 = 1680(16)$ ms and $M_0 = 10.39(12)$ V, with a reduced chi-squared of $\chi_{\text{red}}^2 = 1.42$.

concentration. Though we attempted a power-law fit as suggested by the literature, the data was better described by the logarithmic fit:

$$T_2 = m \ln(c) + T_2^{(0)} \quad (18)$$

where c is the concentration (normalized to be dimensionless), and the two free parameters of the fit are m (the (logarithmic) power at which the T_2 time scales) and $T_2^{(0)}$ (the T_2 time at unit concentration). In particular, $\chi_{\text{red}}^2 = 59.62$ was observed for a power law fit, versus $\chi_{\text{red}}^2 = 25.6$ for the logarithmic fit. The data and fit is depicted in Fig. 13.

We generally observe statistically significant disagreement with the literature values of T_2 . In particular, we

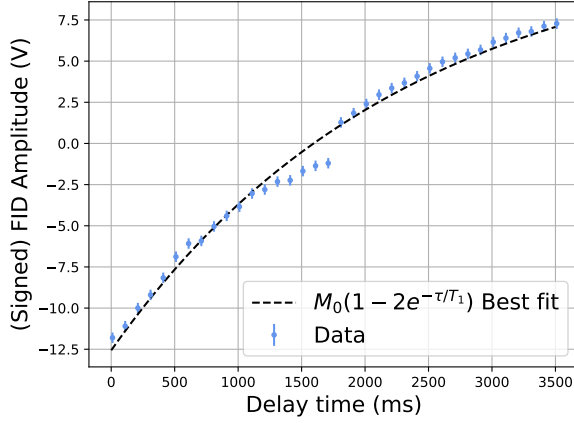


FIG. 12. FID amplitude vs. delay time for $c = 10^{-4}$ mol/L Cu^{2+} concentration solution and associated fit for extracting T_1 . Repetition time was set as 10 seconds. Error bars are statistical. The best fit parameters were $T_1 = 2300(16)$ ms and $M_0 = 12.56(12)$ V, with a reduced chi-squared of $\chi_{\text{red}}^2 = 3.67$.

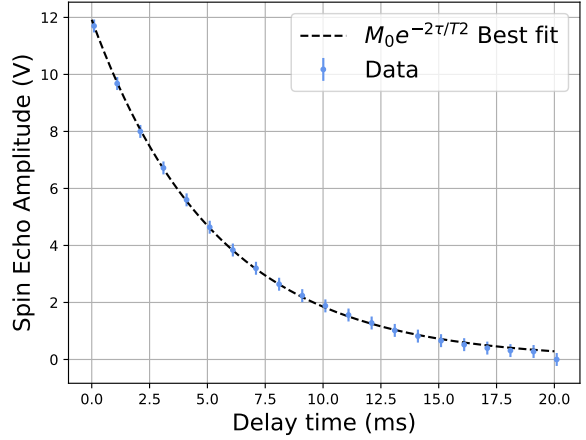


FIG. 14. FID amplitude vs. delay time for $c = 10^{-1}$ mol/L Cu^{2+} concentration solution and associated fit for extracting T_1 . Repetition time was set as 1 second. Error bars are statistical. The best fit parameters were $T_2 = 10.74(24)$ ms and $M_0 = 11.92(17)$ V, with a reduced chi-squared of $\chi_{\text{red}}^2 = 0.13$.

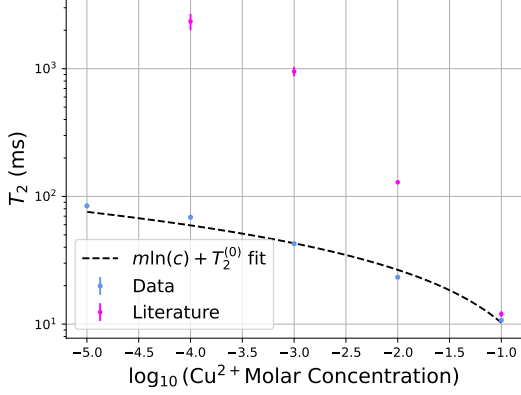


FIG. 13. T_2 relaxation time vs. Copper ion concentration, plotted alongside logarithmic best fit and literature values from [13] (no value was given for $c = 10^{-5}$ mol/L). Error bars are from uncertainties in T_2 fitting parameters for individual concentration curves, and are hidden behind data markers. The best fit parameters were $m = -7.11(13)$ ms and $T_2^{(0)} = -6.11(46)$ ms, with a reduced chi-squared of $\chi_{\text{red}}^2 = 25.6$.

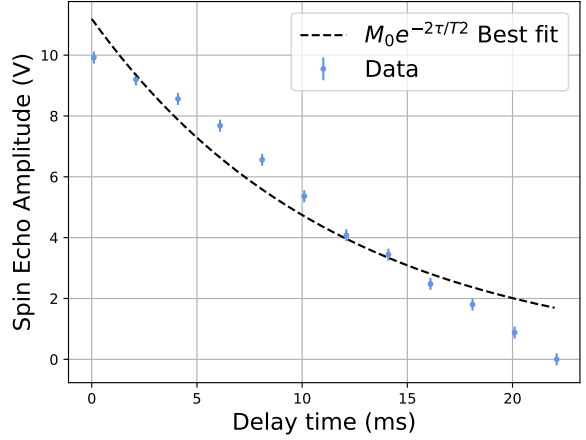


FIG. 15. FID amplitude vs. delay time for $c = 10^{-2}$ mol/L Cu^{2+} concentration solution and associated fit for extracting T_1 . Error bars are statistical. Repetition time was set as 5 seconds. The best fit parameters were $T_2 = 23.31(53)$ ms and $M_0 = 11.19(15)$ V, with a reduced chi-squared of $\chi_{\text{red}}^2 = 22.71$.

observe a very significant deviation from the scaling observed in the literature in the dilute limit. Our value for χ_{red}^2 indicates that the logarithmic power scaling of $m = -7.11(13)$ ms may not be an accurate description of the data and that our uncertainties in T_2 may have been underestimated. However, studying the individual concentration curves across Figs. 14–18, we observe that the individual T_2 values extracted from the fits are not reliable.

With the exception of the $c = 10^{-1}$ curve where the T_2 decay shows a good fit to the data, the data for $c = 10^{-2} - 10^{-5}$ show significant systematic discrepancies compared to the best fit (with $\chi_{\text{red}}^2 \gg 1$). In

particular, for $c = 10^{-2}$ we observe linear as opposed to exponential decay, and for $c = 10^{-3} - 10^{-5}$ we observe a plateau at low-delay times before the amplitude begins to decay exponentially. We have two proposed mechanisms for this discrepancy. First, given that the T_2 time does not appear to saturate to that of water in the dilute limit (we appear to saturate to ~ 100 ms as opposed to the T_2 of water of ~ 2 s that is seen in the literature curve), we suspect the presence of impurities in our samples that may be decreasing the relaxation time. In addition, given the poor fit of the T_2 decay model for dilute concentrations, we suspect that there are other decay mechanisms that the spin-spin interactions may not

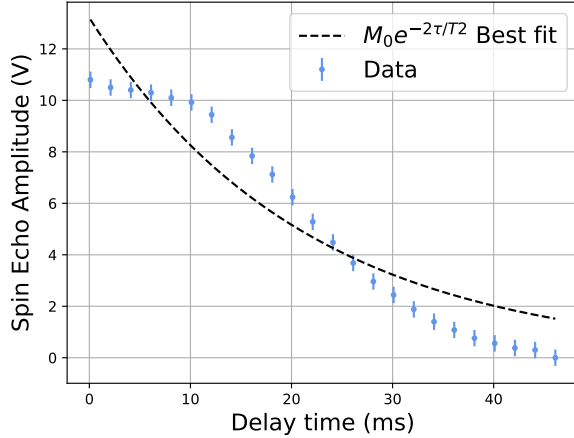


FIG. 16. FID amplitude vs. delay time for $c = 10^{-3}$ mol/L Cu^{2+} concentration solution and associated fit for extracting T_1 . Repetition time was set as 10 seconds. Error bars are statistical. The best fit parameters were $T_2 = 42.61(98)$ ms and $M_0 = 13.20(19)$ V, with a reduced chi-squared of $\chi_{\text{red}}^2 = 18.51$.

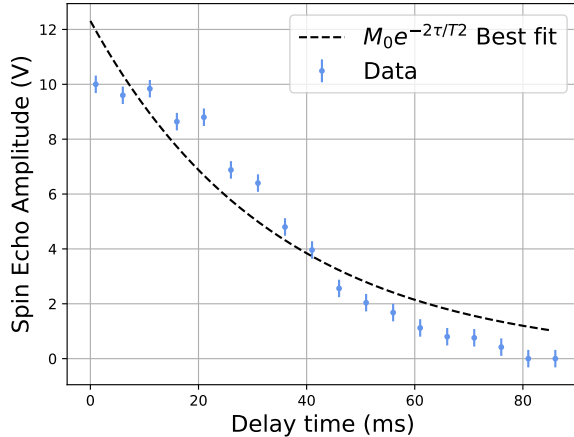


FIG. 17. FID amplitude vs. delay time for $c = 10^{-4}$ mol/L Cu^{2+} concentration solution and associated fit for extracting T_1 . Repetition time was set as 10 seconds. Error bars are statistical. The best fit parameters were $T_2 = 68.6(20)$ ms and $M_0 = 12.31(23)$ V, with a reduced chi-squared of $\chi_{\text{red}}^2 = 13.31$.

be accounting for. In particular, it may be possible that due to incorrect optimization of the 90/180 degree pulses that the dephasing effect of field inhomogeneities may not have been completely compensated for (for example if the 180 degree pulse did not completely invert the spins in the sample), leading to dephasing times that are much lower than anticipated.

VII. CONCLUSIONS

In this paper, we have used pulsed NMR to characterize the gyromagnetic ratios and relaxation times of

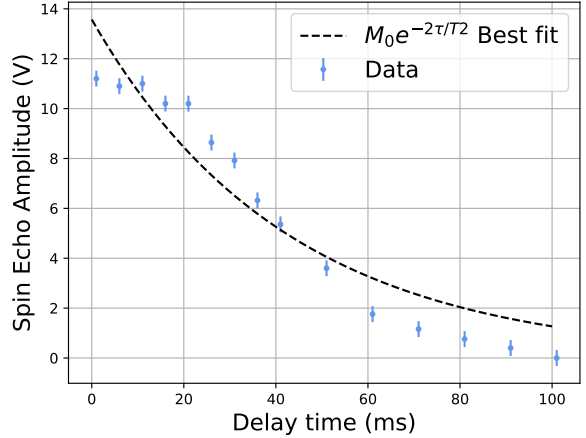


FIG. 18. FID amplitude vs. delay time for $c = 10^{-5}$ mol/L Cu^{2+} concentration solution and associated fit for extracting T_1 . Repetition time was set as 10 seconds. Error bars are statistical. The best fit parameters were $T_2 = 84.4(25)$ ms and $M_0 = 13.57(22)$ V, with a reduced chi-squared of $\chi_{\text{red}}^2 = 17.03$.

glycerine, teflon, and aqueous copper samples. Our measured values for the gyromagnetic ratios of hydrogen and fluoroine (from glycerine and teflon) are of the correct order of magnitude, but are systematically shifted downwards from the accepted literature values [11], indicating an error in our gaussometer calibration. We used the inversion recovery and spin echo methods to characterize the T_1/T_2 times of Glycerine. Although the fits were of good quality, the relaxation times obtained showed statistically significant deviations from the literature values in [12], which we suspect is due to differences in sample purity between the two experiments. Finally, we prepared and characterized the T_1/T_2 times of aqueous copper solution across 10^{-1} - 10^{-5} concentrations. For T_1 extractions, the individual FID amplitude vs. T_1 plots were reasonably well-fit, though contained systematic upward shifts in the amplitude for low concentrations. We conjecture this to be an artifact of insufficient repetition time between pulse sequences. The extracted T_1 times were of the correct order of magnitude, but showed vast deviation from the literature values in [13]. In addition, we observed a poor fit to the proposed power law scaling of T_1 in the ion concentration. For T_2 , we observed that all of the low-concentration spin echo amplitude data were poorly fit by the functional form of the T_2 decay model. Though we attempted a logarithmic fit of T_2 vs. ion concentration based on the shape of the data, the extracted T_2 values severely undershoot the literature values and scaling as predicted in [13]. We suspect that a combination of sample impurity and uncompensated magnetic field inhomogeneities contribute to this discrepancy. A good future direction would be to extract the T_2^* decay time constant from the exponential decay of the FID signal, which is caused by both spin-spin interactions and device specific field-inhomogeneities. If the dephasing times we extract from this method are consis-

tent with our T_2 values as obtained from the spin-echo method, this could suggest that incorrectly compensated field inhomogeneities could be the culprit.

Our results, while plagued with systematic errors, are a good reminder of the importance of carefully tracking systematics and compensations thereof in experimental physics. Though NMR is a widely applicable method for spectroscopy, it is also one that requires care for precise quantitative results - we wish the best of luck for future lab groups on this experiment, and hope that they may learn from our errors

DATA AVAILABILITY

The Jupyter notebook used for data analysis + display of the results can be find in the attached `riopnmr.ipynb` file, submitted along with this report.

ACKNOWLEDGMENTS

I would like to acknowledge my lab partner Heejin Woo - the data collected and presented was taken together. The PHYS 334 lab wiki [10] was used liberally in the structuring of the background of this report.

- [1] N. Bloembergen, E. M. Purcell, and R. V. Pound, Nuclear magnetic relaxation, *Nature* (1947).
- [2] H. Y. Carr and E. M. Purcell, Effects of diffusion on free precession in nuclear magnetic resonance experiments, *Phys. Rev.* **94**, 630 (1954).
- [3] F. Bloch, Nuclear induction, *Phys. Rev.* **70**, 460 (1946).
- [4] E. L. Hahn, Spin echoes, *Phys. Rev.* **80**, 580 (1950).
- [5] S. J. Schmidt, Determination of moisture content by pulsed nuclear magnetic resonance spectroscopy, in *Water Relationships in Foods: Advances in the 1980s and Trends for the 1990s*, edited by H. Levine and L. Slade (Springer US, Boston, MA, 1991) pp. 599–613.
- [6] J. T. Catherine Westbrook, Carolyn Kaut Roth, *MRI in Practice, 4th Edition* (Wiley, 2011).
- [7] In practice a rotating magnetic field is difficult to achieve, and instead a horizontally oscillating magnetic field is used. This is because such a horizontal field can be decomposed into a clockwise and counterclockwise rotating component, and if the clockwise component rotates close to resonance, the effect of the counterclockwise part is negligible.
- [8] J. Sakurai and J. Napolitano, *Modern Quantum Mechanics, 3rd Edition* (Cambridge University Press, 2021).
- [9] At room temperature $k_B T \approx \frac{1}{40}$ eV. The ratio of the two populations is therefore close to one, but is still sufficiently off that a net magnetization could be observed.
- [10] Phys 334 lab wiki (2025).
- [11] K. Herb, Konstantin's gyromagnetic ratio table (2025).
- [12] G. HM., T1 and t2 and complex permittivities of mineral oil, silicone oil, and glycerol at 0.35, 1.5, and 3 t., *Med Phys.* (2019).
- [13] J. Pope and N. Repin, A simple approach to t2 imaging in mri, *Magnetic Resonance Imaging* **6**, 641 (1988).